SCIENCE CHINA
Information Sciences

• RESEARCH PAPER •

June 2026, Vol. 69, Iss. 6, 162201:1–162201:14
https://doi.org/10.1007/s11432-025-4738-4

Distributed adaptive formation with state constraints for multi-agent systems: NE and RNE searching in aggregative games

Zhaoxia PENG[1], Bofan WU[1*], Guoguang WEN[2], Chenyang PAN[3] & Tingwen HUANG[4]

[1]*School of Transportation Science and Engineering, Beihang University, Beijing 100190, China*
[2]*Department of Mathematics, Beijing Jiaotong University, Beijing 100190, China*
[3]*School of Vehicle and Mobility, Tsinghua University, Beijing 100190, China*
[4]*Faculty of Computer Science and Control Engineering, Shenzhen University of Advanced Technology, Shenzhen 518055, China*

Received 25 April 2025/Revised 18 September 2025/Accepted 29 November 2025/Published online 27 January 2026

Abstract A distributed adaptive formation problem with state constraints for multi-agent systems is studied in this article. It can be transformed into an aggregative game, where the local cost function for each agent relies on several aggregate items. Thus, auxiliary variables are employed to estimate these system-wide aggregate items under a distributed communication topology, and a distributed continuous-time Nash equilibrium (NE) seeking strategy is proposed for the multi-agent system to search for an NE point in the aggregative game. Furthermore, the uniqueness of the NE point is analyzed, which depends on the common state constraint set. Considering an extra property of the NE point, a concept of robust NE (RNE) point is first introduced in this paper. The multi-agent system located at the RNE point has the ability to be maintained within the common state constraint set as much as possible under disturbances. For general convex state constraints, an RNE searching algorithm is proposed with a distributed proximal continuous-time strategy. The strategy deals with a max-min fair allocation problem with a mixture of discrete and continuous variables and relaxes the condition that the cost function is monotone. Finally, we provide several simulations to demonstrate the theoretical results.

Keywords distributed adaptive formation problem, aggregative game, Nash equilibrium (NE), robust Nash equilibrium (RNE)

Citation Peng Z X, Wu B F, Wen G G, et al. Distributed adaptive formation with state constraints for multi-agent systems: NE and RNE searching in aggregative games. Sci China Inf Sci, 2026, 69(6): 162201, https://doi.org/10.1007/s11432-025-4738-4

1 Introduction

In the last few decades, formation controls have attracted considerable attention in many areas, such as autonomous vehicles and multiple robots [1]. For more than 20 years of research and development, abundant references have focused on time-invariant and time-varying formation configurations [2, 3]. However, in the absence of prior knowledge of the complex environment, the predefined formation configuration rules lack adaptiveness, such as obstacle avoidance or entering into a security region that always imposes constraints on the states of agents. Several technologies, like the artificial potential field (APF) method [4] and geometric-based approach [5], have the ability to display great obstacle avoidance performance or guarantee state constraint by distance-based penalty function and geometric computation. However, these methods lack consideration for the change of the formation configuration, which results in a significant change in the formation configuration, thereby affecting formation stability and operational efficiency. Thus, the investigation of the optimal formation configuration change in the formation control with state constraints is meaningful.

Recently, cooperative games under distributed communication topologies have been extensively investigated. They aim to minimize a sum of local cost functions subjected to different kinds of constraints, including general equality [6], coupling equality [7], and inequality constraints [8]. With the expansion of applications, great attention has been focused on searching for Nash equilibrium (NE) points in non-cooperative games [9, 10], where the local cost functions are dependent not only on individual states but also on others'. The aggregative game, as a typical non-cooperative game, has also been extensively investigated because of its applications in network systems [11]. Because of the existence of aggregate items which depend on all agents' states and are unavailable to each agent directly, observers were employed for each agent, which estimate all agents' states in [12] and the aggregate items

* Corresponding author (email: by1913022@buaa.edu.cn)

directly in [13,14]. In [14], the aggregative game was proposed for the multi-agent system under a strongly connected topology, and was extended to balance and unbalance graphs in [15]. Known by the authors' best efforts, few studies research the formation controls with state constraints as aggregative games to optimize the formation configurations further. Furthermore, the above literature focuses on the convergence of the searching algorithm but lacks further analysis on the property of the NE point, which is significant for formation controls.

Robustness is a significant property for multi-agent systems, which presents an ability to resist uncertainty. In the tracking control with rigorous stability and performance, robust controls are well-established technologies to deal with unknown parameters and time-varying disturbances [16], and internal uncertainty in the robust output regulation problem [17]. In online optimization [18], the robust MPC scheme was utilized to search for an optimal control protocol in the existence of disturbance and/or uncertainty. The distributed robust optimization aims for the optimal solution in the presence of the uncertainty in objective functions [19] or in constraints [20]. However, the above literature mainly focuses on the uncertainty applied to the system model, and researches "maximum safety margin" to analyze the robust performance of the system under disturbance. To the knowledge of authors, few studies involve the analysis of the robustness of the NE point in the aggregative game, which motivates the promotion of this paper.

In this paper, a distributed adaptive formation problem subjected to a common state constraint for a multi-agent system is studied, which can be transformed into a non-cooperative aggregative game to search for the NE point. There are some main contributions.

(1) A distributed continuous-time NE seeking strategy with the Lagrangian multiplier method is proposed to deal with a non-cooperative aggregative game. Compared with the existing studies [12–15], it prevents the introduction of the projection operator, which influences the complexity and computational accuracy of the proposed optimization strategy. This greatly decreases the complexity, especially in the case of general convex constraints.

(2) The uniqueness of the NE point in the non-cooperative aggregative game is analyzed, which depends on the size of the security region established by the common state constraint set. For the sake of the robustness of the multi-agent system further, a concept of robust NE (RNE) point is first introduced in the multi-NE case. In the presence of uncertain disturbances, compared with other NE points, the system located at the RNE point has the ability to stay within the common state constraint as much as possible.

(3) For the general convex state constraints, a distributed RNE searching algorithm is designed to deal with a max-min optimization problem to search for the RNE point with a distributed proximal continuous-time strategy. Compared with [21], this paper relaxes a strong hypothesis that the local cost function is strictly monotone.

The rest of this article is structured as follows. Section 2 introduces the preliminaries and problem statement. The main result of the distributed continuous-time NE seeking strategy is proposed in Section 3. The concept of RNE is presented and an RNE searching algorithm for the general convex constraint is presented in Section 4. Finally, the simulations are presented in Section 5 and the conclusion is provided in Section 6.

Notations: In this paper, I_m denotes the $m \times m$ identity matrix, $\mathbf{0}_m = [0, 0, \ldots, 0]^{\mathrm{T}} \in \mathbb{R}^m$, and $\lambda_{\max}(\cdot)$ represents the maximum eigenvalue of the matrix. For an integer $k > 0$, let $[k]$ be the index set $\{1, ..., k\}$. Define the concatenated column vector $\mathrm{col}(x_1, ..., x_m) = (x_1^{\mathrm{T}}, ..., x_m^{\mathrm{T}})^{\mathrm{T}}$ for any vector $x_i \in \mathbb{R}^m$. The symbol $\otimes$ denotes the Kronecker product, an operator $(\cdot)^+ = \max\{\cdot, 0\}$, and $\|\cdot\|$ is the Euclidean norm.

2 Preliminaries and problem statement

In this section, some mathematical preliminaries are provided first, and then we describe the adaptive formation problem with state constraints briefly.

2.1 Graph theory

Let a triplet $\mathcal{G} = (\mathcal{V}, \mathcal{E}, \mathcal{A})$ be an undirected graph, where $\mathcal{V} = \{1, 2, \ldots, m\}$ is a node set, $\mathcal{E} \subseteq \mathcal{V} \times \mathcal{V}$ is an edge set and $\mathcal{A} = [a_{ij}] \in \mathbb{R}^{m \times m}$ is an adjacency matrix. An edge $(i, j) \in \mathcal{E}$ holds $(j, i) \in \mathcal{E}$, and the ith agent and jth agent are neighbors and can receive information from each other. Furthermore, the adjacency matrix $\mathcal{A} = [a_{ij}] \in \mathbb{R}^{m \times m}$ is defined as $a_{ij} = 1$ if $(i, j) \in \mathcal{E}$, or $a_{ij} = 0$ otherwise. Since there does not exist self-loop, $a_{ii} = 0$, $\forall i \in [m]$. For the Laplacian matrix associated with $\mathcal{G}$, $\mathcal{L} = [l_{ij}] \in \mathbb{R}^{m \times m}$ is determined as $l_{ii} = \sum_{j=1}^{m} a_{ij}$ and $l_{ij} = -a_{ij}$ for $i \neq j$.

2.2 Convex optimization

A function $f(x) : \mathbb{R}^s \to \mathbb{R}$ is convex, if and only if, for any $x_1, x_2 \in \mathbb{R}^s$ and $0 \leqslant \theta \leqslant 1$, $f(\theta x_1 + (1 - \theta) x_2) \leqslant \theta f(x_1) + (1 - \theta) f(x_2)$. For a lower semi-continuous convex function $f(x)$, a proximal operator $prox_f[p] = \arg\min_x \{f(x) +$

$\frac{1}{2}\|x-p\|^2\}$. Let $\partial f(x)$ denote the sub-differential of $f(x)$. When $f(x)$ is convex and $\partial f(x)$ is monotone, it holds $(q_{x_1}-q_{x_2})^{\mathrm{T}}(x_1-x_2)\geqslant 0$ for all $x_1,x_2\in\mathbb{R}^s$, where $q_{x_1}\in\partial f(x_1)$ and $q_{x_2}\in\partial f(x_2)$. Additionally, the proximal operator $prox_f[\cdot]$ is firmly non-expansive, and $p-x\in\partial f(x)$, if $x=prox_f[p]$. For the indicator function $I_\Omega(\cdot)$ of a closed convex set Ω, such that $I_\Omega(x)=0$ if $x\in\Omega$, or $I_\Omega(x)=\infty$ otherwise, it holds $prox_{I_\Omega}[p]=P_\Omega[p]$, where the projection operator $P_\Omega[p]=\arg\min_{x\in\Omega}\|x-p\|$.

2.3 Problem formulation

In this paper, we consider a multi-agent system with m agents under an undirected graph $\mathcal{G}$. The dynamic model for the multi-agent system is formulated as

$$\dot{x}_i=u_i,\ i\in[m], \tag{1}$$

where $x_i\in\mathbb{R}^s$ is the state of the ith agent and $u_i\in\mathbb{R}^s$ is the input of the ith agent.

In the operation process, the multi-agent system commonly maintains a predefined formation configuration. Since the complexity of the environment, the multi-agent system often needs to modify the formation configuration adaptively based on the environment, such as entering the designated area to ensure the safety of the system. However, it is inappropriate to arbitrarily change the formation configuration, because a large change in the formation configuration not only causes a loss of system energy, but also affects the operational efficiency. Thus, an adaptive constrained formation problem for a multi-agent system is formulated as follows:

$$\begin{aligned}&\min f_i(x)=\frac{1}{m}\sum_{k=1}^{m}\|x_i-d_i-x_k+d_k\|^2,\\&\text{s.t.}\ \ x_i\in\Omega,\end{aligned} \tag{2}$$

where $x=\mathrm{col}(x_1,...,x_m)$, $d=\mathrm{col}(d_1,...,d_m)$ represents a predefined formation, and d_i is the relative position of the ith agent in the predefined formation. The symbol Ω represents the common state constraint set, such as $\Omega=\{\mathbf{x}\in\mathbb{R}^s|g_p(\mathbf{x})\leqslant 0,p\in[n]\}$. It is a designated security region enclosed by inequalities $g_p(x)\leqslant 0,p\in[n]$. Thus, in the optimization problem (2), the predefined formation configuration is regarded as the benchmark for evaluating the optimality of the formation configuration, and the formation configuration for the multi-agent system is modified with minimal changes adaptively based on the common state constraint set Ω.

Assumption 1. The common state constraint Ω is compact and convex.

Assumption 2. The undirected communication topology graph $\mathcal{G}$ is connected.

Remark 1. In the complex environment, it is necessary for the multi-agent system to change its predefined formation configuration adaptively relying on the size of the security region established by the common state constraint set. To reduce the energy loss and the formation instability, each agent focuses on the change of the formation configuration further. In this paper, the change of the formation configuration depends on the average of deviations between the actual distances, i.e., x_i-x_k, and the predefined distances, i.e., d_i-d_k, for every two ith and kth agents. Compared with fixed formation configuration rules in [2, 3], this optimization-based approach can modify the formation configuration adaptively for the multi-agent system based on the information of the common state constraint set Ω.

Remark 2. Compared with the containment problem [22], the adaptive constrained formation problem in (2) has several discrepancies. (1) The common state constraint set is established based on the real-time environment information. (2) The multi-agent system is required to search for an optimal formation configuration within the common state constraint set, rather than forming a fixed formation configuration which is dependent on the weight of the communication.

Accordingly, the optimization problem (2) holds

$$f_i(x)=\|x_i-d_i\|^2+\upsilon(x)-2(x_i-d_i)^{\mathrm{T}}s(x), \tag{3}$$

where $s(x)=\frac{1}{m}\sum_{k=1}^{m}s_k(x_k)$ and $\upsilon(x)=\frac{1}{m}\sum_{i=k}^{m}\upsilon_k(x_k)$ are two aggregate functions with $s_k(x_k)=x_k-d_k$ and $\upsilon_k(x_k)=\|x_k-d_k\|^2$. Thus, the function $f_i(x)$ is related to three variables, i.e., x_i, $s(x)$ and $\upsilon(x)$, and can be expressed as $J_i(x_i,s(x),\upsilon(x))$. Thus, the problem (2) is equivalent to an aggregative game formalized as follows:

$$\begin{aligned}&\min_{x_i} J_i(x_i,s(x),\upsilon(x)),\\&\text{s.t.}\ \ x_i\in\Omega.\end{aligned} \tag{4}$$

For the aggregative game (4), it satisfies several properties which are proposed as mild hypothesises in [15].

Property 1. The cost function $J_i(x_i, s(x), \upsilon(x))$ is convex with respect to x_i.

Property 2. The cost function $J_i(x_i, s(x), \upsilon(x))$ is Lipschitz continuous.

Property 3. An NE point x^* of the aggregative game (4) satisfies

$$J_i(x_i, s(x_i, x^*_{-i}), \upsilon(x_i, x^*_{-i})) \geqslant J_i(x^*_i, s(x^*), \upsilon(x^*)), \tag{5}$$

for all $x_i \in \Omega$, $i \in [m]$, where $x_{-i} = \mathrm{col}(x_1, x_2, ..., x_{i-1}, x_{i+1}, ..., x_m)$.

3 Distributed continuous-time NE seeking strategy

In this section, a distributed continuous-time NE seeking strategy is designed for the aggregative game (4) under an undirected communication topology graph $\mathcal{G}$ as follows:

$$\begin{aligned}
&\dot{\chi} = -\chi - (L \otimes I_{s+1})\chi - (L \otimes I_{s+1})\eta + \gamma(x),\\
&\dot{\eta} = \chi,\\
&\dot{x} = \frac{1}{4}(-\nabla_x J(x, E_1\chi, E_2\chi) - \nabla_x g(x)^{\mathrm{T}}(\zeta + g(x))^+),\\
&\dot{\zeta} = \frac{1}{2}(-\zeta + (\zeta + g(x))^+),
\end{aligned} \tag{6}$$

where $\chi = \mathrm{col}(\chi_1, ..., \chi_m)$ with $\chi_i \in \mathbb{R}^{s+1}$, $\eta = \mathrm{col}(\eta_1, ..., \eta_m)$ with $\eta_i \in \mathbb{R}^{s+1}$, $\gamma(x) = \mathrm{col}(\gamma_1(x_1), ..., \gamma_m(x_m))$ with $\gamma_i(x_i) = \mathrm{col}(s_i(x_i), \upsilon_i(x_i)) \in \mathbb{R}^{s+1}$, $g(x) = \mathrm{col}(g(x_1), ...g(x_m))$ with $g(x_i) = \mathrm{col}(g_1(x_i), ..., g_n(x_i)) \in \mathbb{R}^n$, $\zeta = \mathrm{col}(\zeta_1, ..., \zeta_m)$ with $\zeta_i \in \mathbb{R}^n$, $\nabla_x J(x, E_1\chi, E_2\chi) = \mathrm{col}(\nabla_{x_1} J_1(x_1, e_1\chi_1, e_2\chi_1), ..., \nabla_{x_m} J_m(x_m, e_1\chi_m, e_2\chi_m))$ with $\nabla_{x_i} J_i(x_i, e_1\chi_i, e_2\chi_i) = \nabla_{x_i} J_i(x_i, s(x), \upsilon(x))|_{s(x)=e_1\chi_i, \upsilon(x)=e_2\chi_i}$, two augmented vectors $E_1 = I_m \otimes e_1$ and $E_2 = I_m \otimes e_2$ with $e_1 = [I_s, \mathbf{0}_s]$ and $e_2 = [\mathbf{0}_s^{\mathrm{T}}, 1]$, and $\nabla_x g(x) = \mathrm{col}(\nabla_{x_1} g(x_1), ..., \nabla_{x_m} g(x_m))$.

Remark 3. The optimization problem (4) can be regarded as a potential game. However, compared with [23] about the distributed potential game, the aggregate functions $s(x)$ and $\upsilon(x)$ are unavailable to each agent directly. Thus, the observer χ is designed to obtain these system-wide variables and is utilized to generate the gradient.

Next, we present several lemmas and a theorem for the effectiveness of strategy (6).

Lemma 1. Suppose Assumption 2 holds. For any initial state of $(\chi(0), \eta(0))$, the trajectory $(\chi(t), (\mathcal{L} \otimes I_{s+1})\eta(t))$ generated by (6) converges to a stable equilibrium point $(\mathbf{1}_m \otimes \frac{\sum_{i=1}^m \gamma_i(x_i)}{m}, \gamma(x) - \mathbf{1}_m \otimes \frac{\sum_{i=1}^m \gamma_i(x_i)}{m})$.

Proof. Since the communication topology graph $\mathcal{G}$ for the multi-agent system is undirected, it is a special directed balance graph, and the details of the proof can refer to [15].

Lemma 2. Suppose Assumption 1 holds. If and only if $(\chi^*, \eta^*, x^*, \zeta^*)$ is an equilibrium point of (6), then x^* is an NE point in (4) with ζ^* being the dual optimal solution.

Proof. For the aggregative game (4), define the Lagrangian function as

$$L_i = J_i(x_i, s(x), \upsilon(x)) + \zeta_i^{\mathrm{T}} g(x_i). \tag{7}$$

Since the strong duality property holds [24], $\bar{x}^*_i$ is the NE point in the aggregative game (4), if and only if there exists $\bar{\zeta}^*_i$, such that $(\bar{x}^*_i, \bar{\zeta}^*_i)$ satisfies the KKT conditions as follows:

$$\begin{aligned}
&\nabla_{x_i} J_i(\bar{x}^*_i, s(\bar{x}^*), \upsilon(\bar{x}^*)) + \nabla_{x_i} g(\bar{x}^*_i)^{\mathrm{T}} \bar{\zeta}^*_i = \mathbf{0}_s,\\
&g(\bar{x}^*_i) \leqslant \mathbf{0}_n, \qquad \bar{\zeta}^*_i \geqslant \mathbf{0}_n,\\
&\bar{\zeta}^{*\mathrm{T}}_i g(\bar{x}^*_i) = 0, \qquad \forall i \in [m].
\end{aligned} \tag{8}$$

Assume $(\chi^*, \eta^*, x^*, \zeta^*)$ is an equilibrium point in the strategy (6). Based on Lemma 1, it holds $\chi^* = \mathbf{1}_m \otimes \frac{\sum_i \gamma_i(x^*_i)}{m}$ and the two items $E_1\chi^* = \mathbf{1}_m \otimes \frac{\sum_i s_i(x^*_i)}{m}$ and $E_2\chi^* = \mathbf{1}_m \otimes \frac{\sum_i \upsilon_i(x^*_i)}{m}$. Thus, we obtain

$$\begin{aligned}
\mathbf{0}_{sm} &= -\nabla_x J(x^*, E_1\chi^*, E_2\chi^*) - \nabla_x g(x^*)^{\mathrm{T}}(\zeta^* + g(x^*))^+,\\
\zeta^* &= (\zeta^* + g(x^*))^+.
\end{aligned} \tag{9}$$

Based on the first equation, it holds $\mathbf{0}_{sm} = -\mathrm{col}(\nabla_{x_1} J(x^*_1, s(x^*), \upsilon(x^*)) - \nabla_{x_1} g(x^*_1)^{\mathrm{T}} \zeta^*_1, ..., \nabla_{x_m} J(x^*_m, s(x^*), \upsilon(x^*)) - \nabla_{x_m} g(x^*_m)^{\mathrm{T}} \zeta^*_m)$. Moreover, since the second equation, i.e., $\zeta^* = (\zeta^* + g(x^*))^+$, is equivalent to the complementary slackness conditions (9), the equilibrium point $(\chi^*, \eta^*, x^*, \zeta^*)$ satisfies the KKT optimality conditions (8) and (9). Thus, if and only if $(\chi^*, \eta^*, x^*, \zeta^*)$ is an equilibrium point of the strategy (6), then x^* is an NE point in the aggregative game (4) with ζ^* being the dual optimal solution.

Theorem 1. Suppose Assumptions 1 and 2 hold. The trajectory $(\chi(t), \eta(t), x(t), \zeta(t))$ associated with the distributed continuous-time NE searching strategy (6) is bounded for any $t \in \mathbb{R}^+$, and $x(t)$ converges to the NE point of the optimization problem (4).

Proof. Let $\psi(x,\zeta) = \sum_{i=1}^m J_i(x_i, s(x), \upsilon(x)) + \frac{1}{2}\|\kappa(x,\zeta)\|^2$ with $\kappa(x,\zeta) = (\zeta + g(x))^+$, and define the Lyapunov function as follows:

$$\begin{aligned} V = &- (x-x^*)^{\mathrm{T}}(\nabla_x g^{\mathrm{T}}(x^*)\kappa(x^*,\zeta^*)) - (x-x^*)^{\mathrm{T}}\left(\nabla_x \sum_{i=1}^m J_i^*\right) - (\zeta-\zeta^*)^{\mathrm{T}}\kappa(x^*,\zeta^*) \\ &+ \psi(x,\zeta) - \psi(x^*,\zeta^*) + (x-x^*)^{\mathrm{T}}\left(2I_{sm} - \frac{\mathcal{L}_c \otimes I_s}{m}\right)(x-x^*) + \frac{1}{2}\|\zeta-\zeta^*\|^2, \end{aligned} \tag{10}$$

where

$$\nabla_x \sum_{i=1}^m J_i^* = \nabla_x J^* + \frac{2}{m}(\mathcal{L}_c \otimes I_s)(x^* - d)$$

with

$$\nabla_x J^* = \begin{bmatrix} \nabla_{x_1} J_1(x_1^*, s(x^*), \upsilon(x^*)) \\ \dots \\ \nabla_{x_m} J_m(x_m^*, s(x^*), \upsilon(x^*)) \end{bmatrix},$$

and $\mathcal{L}_c \in \mathbb{R}^{m\times m}$ being the Laplacian matrix of a complete topology. Since $\psi(x,\zeta)$ is convex, it holds $\psi(x,\zeta) - \psi(x^*,\zeta^*) - (x-x^*)^{\mathrm{T}}(\nabla_x \sum_{i=1}^m J_i^* + \nabla_x g^{\mathrm{T}}(x^*)\kappa(x^*,\zeta^*)) - (\zeta-\zeta^*)^{\mathrm{T}}\kappa(x^*,\zeta^*) \leqslant 0$. Because $\lambda_{\max}(\mathcal{L}_c) = m$, it holds

$$V \geqslant (x-x^*)^{\mathrm{T}}\left(2I_{sm} - \frac{\mathcal{L}_c \otimes I_s}{m}\right)(x-x^*) + \frac{1}{2}\|\zeta-\zeta^*\|^2 \geqslant 0, \tag{11}$$

and $V = 0$, iff $(\chi, \eta, x, \zeta) = (\chi^*, \eta^*, x^*, \zeta^*)$. Thus, the Lyapunov function is positive definite. Furthermore, based on (8) and (9), the derivative of Lyapunov function V satisfies

$$\begin{aligned} \dot{V} = &\frac{1}{2}(\kappa(x,\zeta) - \kappa(x^*,\zeta^*) + \zeta - \zeta^*)^{\mathrm{T}}(-\zeta + \kappa(x,\zeta)) + (x-x^*)^{\mathrm{T}}(-\nabla_x J - \nabla_x g^{\mathrm{T}}(x)\kappa(x,\zeta)) \\ &+ \frac{1}{4}(\nabla_x J + \nabla_x g^{\mathrm{T}}(x)\kappa(x,\zeta) + 2(x-x^*))^{\mathrm{T}}(-\nabla_x \bar{J} + \nabla_x J) \\ &+ \frac{1}{4}(\nabla_x J + \nabla_x g^{\mathrm{T}}(x)\kappa(x,\zeta))^{\mathrm{T}}(-\nabla_x J - \nabla_x g^{\mathrm{T}}(x)\kappa(x,\zeta)), \end{aligned} \tag{12}$$

where $\nabla_x \bar{J}$ is the abbreviation of $\nabla_x J(x, E_1\chi, E_2\chi)$. Define the sum of the first two items in (12) as δ_1. Noting that $\nabla_x J^* + \nabla_x g(x^*)^{\mathrm{T}}\zeta^* = 0$, it holds

$$\delta_1 = (x-x^*)^{\mathrm{T}}(-\nabla_x J + \nabla_x J^*) + \delta_2, \tag{13}$$

where $\delta_2 = \frac{1}{2}(\kappa(x,\zeta) - \kappa(x^*,\zeta^*) + \zeta - \zeta^*)^{\mathrm{T}}(-\zeta + \kappa(x,\zeta)) + (x-x^*)^{\mathrm{T}}(-\nabla_x g(x)^{\mathrm{T}}\kappa(x,\zeta) + \nabla_x g(x^*)^{\mathrm{T}}\zeta^*)$. Moreover, since $\zeta^* = \kappa(x^*,\zeta^*)$, it follows that

$$\begin{aligned} \delta_2 = &- (x-x^*)^{\mathrm{T}}(\nabla_x g(x)^{\mathrm{T}}\kappa(x,\zeta) - \nabla_x g(x^*)^{\mathrm{T}}\zeta^*) - \frac{1}{2}\|\zeta - \kappa(x,\zeta)\|^2 \\ &+ (\kappa(x,\zeta) - \zeta^*)^{\mathrm{T}}(-\zeta + \kappa(x,\zeta)). \end{aligned} \tag{14}$$

Furthermore, since $-\zeta + \kappa(x,\zeta) = g(x) + \hat{\kappa}(x,\zeta)$, where $\hat{\kappa}(x,\zeta) = (-\zeta - g(x))^+$, it gets

$$\begin{aligned} \delta_2 = &- \kappa(x^*,\zeta^*)^{\mathrm{T}}(g(x) - g(x^*) - \nabla_x g^{\mathrm{T}}(x^*)(x-x^*)) - \kappa(x^*,\zeta^*)^{\mathrm{T}}(g(x^*) + \hat{\kappa}(x,\zeta)) \\ &+ \kappa(x,\zeta)^{\mathrm{T}}(g(x) - g(x^*) - \nabla_x g^{\mathrm{T}}(x)(x-x^*)) + \kappa(x,\zeta)^{\mathrm{T}}(g(x^*) + \hat{\kappa}(x,\zeta)) \end{aligned}$$

$$- \frac{1}{2}\|\zeta - \kappa(x, \zeta)\|^2. \tag{15}$$

Because of two nonnegativity items $\kappa(x, \zeta)$ and $\kappa(x^*, \zeta^*)$, and the convexity of $g(x)$, the first and third items in (15) are nonpositive. Since x^* is an optimal solution in the aggregative game (4), it gets $\kappa(x, \zeta)^{\mathrm{T}} g(x^*) \leqslant 0$ and $\kappa(x^*, \zeta^*)^{\mathrm{T}} g(x^*) = 0$. Furthermore, $\kappa(x, \zeta)^{\mathrm{T}} \hat{\kappa}(x, \zeta) = 0$ and $-\kappa(x^*, \zeta^*)^{\mathrm{T}} \hat{\kappa}(x, \zeta) \leqslant 0$. Thus, the first two items in (15) are also nonpositive. Thus, we obtain

$$\delta_2 \leqslant -\frac{1}{2}\|\zeta - \kappa(x, \zeta)\|^2. \tag{16}$$

Submitting (16) into (12) yields

$$\begin{aligned} \dot{V} \leqslant\ & \frac{1}{4}(\nabla_x J + \nabla_x g^{\mathrm{T}}(x)\kappa(x, \zeta) + 2(x - x^*))^{\mathrm{T}}(-\nabla_x \bar{J} + \nabla_x J) - \frac{1}{2}\|\zeta - \kappa(x, \zeta)\|^2 \\ & + (x - x^*)^{\mathrm{T}}(-\nabla_x J + \nabla_x J^*) - \frac{1}{4}\|\nabla_x J + \nabla_x g^{\mathrm{T}}(x)\kappa(x, \zeta)\|^2. \end{aligned} \tag{17}$$

Based on Lemma 1, the two items $E_1\chi$ and $E_2\chi$ converge to $\mathbf{1}_m \otimes \frac{\sum_i s_i(x_i)}{m}$ and $\mathbf{1}_m \otimes \frac{\sum_i v_i(x_i)}{m}$, which implies $\nabla_x \bar{J} \to \nabla_x J$. Thus, there exists a constant T such that $\dot{V}$ is bounded when $t \leqslant T$, and $\dot{V} \leqslant 0$ when $t \geqslant T$. Moreover, there exists a strongly positive invariant and bounded set $M_0 \triangleq \{(\chi, \eta, x, \zeta) \in \mathbb{R}^{(s+1)m} \times \mathbb{R}^{(s+1)m} \times \mathbb{R}^{sm} \times \mathbb{R}^{mn} | V \leqslant q\}$ with $q > 0$. Therefore, for any initial point $(\chi(0), \eta(0), x(0), \zeta(0))$, the trajectory $(\chi(t), \eta(t), x(t), \zeta(t))$ based on the strategy (6) is bounded for $t \in \mathbb{R}^+$. According to the LaSalle invariance principle [25], it holds that the trajectory $(\chi(t), \eta(t), x(t), \zeta(t))$ converges to the largest weakly invariant set $\hat{M}_0$ asymptotically, such that $\hat{M}_0 \subseteq M_0 \cap \Xi_0$ with $\Xi_0 = \{(\chi(t), \eta(t), x(t), \zeta(t)) | \dot{V} = 0\}$. For an arbitrary point $(\hat{\chi}, \hat{\eta}, \hat{x}, \hat{\zeta})$ in the set $\hat{M}_0$, it holds that $\dot{V}(\hat{\chi}, \hat{\eta}, \hat{x}, \hat{\zeta}) = 0$. Based on (17), we get $\nabla_x J|_{x=\hat{x}} + \nabla_x g^{\mathrm{T}}(\hat{x})\kappa(\hat{x}, \hat{\zeta}) = 0$, $\hat{\zeta} - \kappa(\hat{x}, \hat{\zeta}) = 0$, and $-\nabla_x \bar{J}|_{x=\hat{x}} + \nabla_x J_{x=\hat{x}} = 0$. Thus, $(\hat{\chi}, \hat{\eta}, \hat{x}, \hat{\zeta})$ is an equilibrium point of (6). In light of Lemma 2, $\hat{x}$ is the optimal solution of (4). Because of the arbitrariness of $(\hat{\chi}, \hat{\eta}, \hat{x}, \hat{\zeta})$, the trajectory $x(t)$ among $(\chi(t), \eta(t), x(t), \zeta(t))$ based on (6) converges to the optimal solution of (4).

Remark 4. Compared with the proposed strategy in [15] which utilizes the projection operator method to guarantee the satisfactory of the common state constraint set, the NE searching strategy (6) employs the Lagrangian multiplier method. Though the introduction of the Lagrangian multipliers results in the high-dimensional state variables, it prevents the model complexity and computational accuracy caused by projection. It is because the projection operator has been used to search for the nearest point within a feasible set to a point, which needs to solve a quadratic programming problem. This greatly increases the complexity, especially in the case of general convex constraints.

Lemma 3. When the security region Ω established by the common state constraint set can accommodate the predefined formation configuration, there exists an infinite number of NE points.

Proof. When the security region Ω established by the common state constraint set can accommodate the prescribed formation configuration, as long as the agents form the predefined formation configuration anywhere within Ω, all the local costs $J_i(x_i, s(x), v(x)) = 0$, $\forall i$. It implies that the multi-agent system is located at an NE point. Thus, there exists an infinite number of NE points in this case.

4 Robust Nash equilibrium point

In this section, we research an extra property of these NE points further and introduce a novel concept, the RNE point. Furthermore, we propose an RNE searching algorithm in the case of a general convex state constraint.

4.1 The concept of RNE

When the multi-NE case appears, the NE point searched by the strategy (6) prefers the frontier of the feasible region Ω. It is because when each agent enters into Ω, the strategy (6) does not impose any force to push the multi-agent system deeper, but emphasizes the formation configuration achievement. However, for a multi-UGV [1] and multi-UAV [2] system, when it enters a security region for resting after a field operation, it prefers to stay in the core of the security region rather than staying around the boundary, because the impact of external disturbance on the multi-agent system located in the core area is minimal. Therefore, it promotes the further study of the robustness property for the multi-agent system and the proposal of a new concept, the RNE point.

Definition 1 (RNE point)**.** When the multi-agent system is located at an NE point, if the agent closest to the boundary is farthest from the boundary of the constraint, then the NE point is the RNE point.

Remark 5. The common state constraint set is established by the agent based on the captured real-time environment information. Since the agent has observation errors during the observation process, it results in the deviation of the common state constraint set. In this case, when the multi-agent system is located at RNE, it can maintain the common state constraint as much as possible.

4.2 An RNE searching algorithm with a general constraint

In this subsection, a general but convex feasible region $\Omega = \{\mathbf{x} | g_p(\mathbf{x}) \leqslant 0, p \in [n]\}$ is further considered. The general RNE searching problem is described as

$$\begin{aligned} &\max_{x} \min_{i,p} \Re_p(x_i, g_p(x_i)), \\ &\quad \text{s.t.} \quad x_i - d_i = x_k - d_k, \quad x_i \in \Omega, \ \forall i,k \in [m], \end{aligned} \tag{18}$$

where $\Re_p(x_i, g_p(x_i))$ is related to the distance between the ith agent and the pth constraint boundary.

Assumption 3. The cost function $\Re_p(x_i, g_p(x_i))$ is twice continuously differentiable and strongly concave with respect to x_i on the common state constraint set Ω.

Furthermore, the problem (18) can be rewritten as

$$\begin{aligned} &\min_{x} \max_{i,p} -\Re_p(x_i, g_p(x_i)) + \sum_{i=1}^{m} I_\Omega(x_i), \\ &\quad \text{s.t.} \quad x_i - d_i = x_k - d_k, \ \forall i,k \in [m]. \end{aligned} \tag{19}$$

Remark 6. For the indicator function I_Ω, it requires a prerequisite that the initial states of all agents must be within Ω. Fortunately, in this paper, since there exists an additional step first to search for an NE point which is within Ω, the introduction of the indicator is appropriate.

Despite the constraint and objective of the problem (19) being both convex, the mixture of the optimized variables results in the traditional optimization technology being invalid. To remedy it, we employ an auxiliary variable r_1 to measure the maximal metric for $-\Re_p(x_i, g_p(x_i))$, and the problem (19) is redescribed as

$$\begin{aligned} &\min_{x, r_1} \ r_1 + \sum_{i=1}^{m} I_\Omega(x_i), \\ &\text{s.t.} \ x_i - d_i = x_k - d_k, \qquad \forall i,k \in [m], \\ &\quad - \Re_p(x_i, g_p(x_i)) \leqslant r_1, \forall i \in [m], \ p \in [n]. \end{aligned} \tag{20}$$

Inspired by [26], we employ logarithmic barrier functions to relax the problem (20) as

$$\begin{aligned} &\min_{x, r_1} \ \tau r_1 + \sum_{i=1}^{m} I_\Omega(x_i) - \sum_{i=1}^{m} \sum_{p=1}^{n} \log(r_1 + \Re_p(x_i, g_p(x_i))), \\ &\text{s.t.} \ x_i - d_i = x_k - d_k, \ \forall i,k \in [m], \end{aligned} \tag{21}$$

where τ is an adaptive inverse log-barrier scaler.

Remark 7. The constraint $-\Re_p(x_i, g_p(x_i)) \leqslant r_1$ is softened as an extra penalty and the adaptive scaler parameter τ weights the two items in the cost function (21). In [26], the update rule of τ is linear growth. Sometimes, a large constant τ is enough to restrict the deviation between the optimal solutions in problems (20) and (21) within an appropriate tolerance.

Similarly, by copying the global parameter r_1 as r_{1i} for the ith agent, the optimization problem (21) is rewritten as

$$\begin{aligned} &\min_{x, \bar{r}_1} \frac{\tau}{m} \sum_{i=1}^{m} r_{1i} + \sum_{i=1}^{m} I_\Omega(x_i) - \sum_{i=1}^{m} \sum_{p=1}^{n} \log(r_{1i} + \Re_p(x_i, g_p(x_i))), \\ &\text{s.t.} \ \ x_i - d_i = x_k - d_k, \quad r_{1i} = r_{1k}, \ \forall i,k \in [m], \end{aligned} \tag{22}$$

where $\bar{r}_1 = \mathrm{col}(r_{11}, ..., r_{1m}) \in \mathbb{R}^m$. The Lagrangian function is described as

$$\bar{L} = h(x, \bar{r}_1) + \alpha \Upsilon^{\mathrm{T}} (\mathcal{L} \otimes I_s)(x - d) + \beta \Psi^{\mathrm{T}} (\mathcal{L} \otimes I_1) \bar{r}_1 \tag{23}$$

with two positive constants α and β, $\Upsilon = \mathrm{col}(\upsilon_1, ..., \upsilon_m) \in \mathbb{R}^{sm}$, $\Psi = \mathrm{col}(\psi_1, ..., \psi_m) \in \mathbb{R}^m$ and $h(x, \bar{r}_1) = \sum_{i=1}^m h_i(x_i, r_{1i})$, such as $h_i(x_i, r_{1i}) = h_i^1(x_i, r_{1i}) + h_i^2(x_i)$, where $h_i^1(x_i, r_{1i}) = \frac{\tau}{m} r_{1i} - \sum_{p=1}^n \log(r_{1i} + \Re_p(x_i, g_p(x_i)))$ and $h_i^2(x_i) = I_\Omega(x_i)$. The KKT conditions hold

$$\begin{aligned}
&\mathbf{0}_m = \nabla_{\bar{r}_1} h^1(x^*, \bar{r}_1^*) + \beta (\mathcal{L} \otimes I_1) \Psi^*, \\
&\mathbf{0}_{sm} \in \nabla_x h^1(x^*, \bar{r}_1^*) + \partial_x h^2(x^*) + \alpha (\mathcal{L} \otimes I_s) \Upsilon^*, \\
&\mathbf{0}_{sm} = (\mathcal{L} \otimes I_s)(x^* - d), \\
&\mathbf{0}_m = (\mathcal{L} \otimes I_1) \bar{r}_1^*,
\end{aligned} \tag{24}$$

where $h^1(x, \bar{r}_1) = \sum_{i=1}^m h_i^1(x_i, r_{1i})$ and $h^2(x) = \sum_{i=1}^m h_i^2(x_i)$.

A distributed continuous-time RNE searching strategy for a general constraint is designed as follows:

$$\begin{aligned}
&\dot{\bar{r}}_1 = -\nabla_{\bar{r}_1} h^1(x, \bar{r}_1) - \beta (\mathcal{L} \otimes I_1) \Psi - \beta (\mathcal{L} \otimes I_1) \bar{r}_1, \\
&\dot{x} = prox_{h^2}[x - \ell - \alpha (\mathcal{L} \otimes I_s)(x - d)] - x, \\
&\dot{\Upsilon} = \alpha (\mathcal{L} \otimes I_s)(x - d), \\
&\dot{\Psi} = \beta (\mathcal{L} \otimes I_1) \bar{r}_1, \\
&\dot{\tau} = c,
\end{aligned} \tag{25}$$

where $\ell = \nabla_x h^1(x, \bar{r}_1) + \alpha (\mathcal{L} \otimes I_s) \Upsilon$.

Remark 8. In the general convex state constraint case, the optimization problem (22) contains the term $\sum_{i=1}^m I_\Omega(x_i)$, which results in the existence of non-differentiable points. Thus, the gradient-based method is not applicable, and the proposed distributed continuous-time RNE searching strategy (25) needs to utilize the proximal operator $prox_f[\cdot]$.

Lemma 4. For a positive constant τ, if there is an equilibrium point $(x^*, \bar{r}_1^*, \Upsilon^*, \Psi^*)$ of the strategy (25), then $(x^*, \bar{r}_1^*)$ is the optimal solution of the problem (22) and (Υ_i^*, Ψ_i^*) is the optimal solution of the dual problem.

Proof. Let $(x^*, \bar{r}_1^*, \Upsilon^*, \Psi^*)$ denote an equilibrium point of the strategy (25). Thus, it holds

$$\begin{aligned}
&\mathbf{0}_m = -\nabla_{\bar{r}_1} h^1(x^*, \bar{r}_1^*) - \beta (\mathcal{L} \otimes I_1) \Psi^* - \beta (\mathcal{L} \otimes I_1) \bar{r}_1^*, \\
&\mathbf{0}_{sm} = prox_{h^2}[x^* - \ell^* - \alpha (\mathcal{L} \otimes I_s)(x^* - d)] - x^*, \\
&\mathbf{0}_{sm} = \alpha (\mathcal{L} \otimes I_s)(x^* - d), \\
&\mathbf{0}_m = \beta (\mathcal{L} \otimes I_1) \bar{r}_1^*.
\end{aligned} \tag{26}$$

Furthermore, the second equation in (26) holds $\mathbf{0}_{sm} \in \partial_x h^2(x^*) + \ell^*$. Based on the KKT conditions (24), we obtain that $(x^*, \bar{r}_1^*)$ is still the optimal solution of the problem (22) and (Υ_i^*, Ψ_i^*) is the optimal solution of its dual problem.

Theorem 2. Suppose Assumption 2 holds. For a positive constant τ and any feasible initial state $(x(0), \bar{r}_1(0), \Upsilon(0), \Psi(0)) \in \mathbb{R}^{sm} \times \mathbb{R}^m \times \mathbb{R}^{sm} \times \mathbb{R}^m$ satisfying $\Re_p(x_i(0), g_p(x_i(0)))^2 \leqslant r_{1i}$, $\forall i \in [m]$, $p \in [n]$, then the trajectory $(x(t), \bar{r}_1(t), \Upsilon(t), \Psi(t))$ with respect to (25) is bounded for $t \geqslant 0$, if $0 < \alpha < \frac{1}{\lambda_{\max}(\mathcal{L})}$ and $0 < \beta < \frac{1}{\lambda_{\max}(\mathcal{L})}$. Furthermore, $(x(t), \bar{r}_1(t))$ converges to the optimal solution of the optimization problem (22).

Proof. Let $(x^*, \bar{r}_1^*, \Upsilon^*, \Psi^*)$ be an equilibrium point of (25). Define the Lyapunov function as follows:

$$V_2 = \varpi_1 + \varpi_2 + \varpi_3, \tag{27}$$

where

$$\begin{aligned}
&\varpi_1 = \frac{1}{2} \|\vartheta - \vartheta^*\|^2 + \frac{1}{2} \|\Xi - \Xi^*\|^2, \\
&\varpi_2 = \vartheta^{\mathrm{T}} \mathcal{L}_\sigma (\Xi - \Xi^*) + \frac{1}{2} \vartheta^{\mathrm{T}} \mathcal{L}_\sigma \vartheta, \\
&\varpi_3 = H^1(\vartheta) - H^1(\vartheta^*) - (\vartheta - \vartheta^*)^{\mathrm{T}} \nabla_\vartheta H^1(\vartheta^*)
\end{aligned}$$

with $\mathcal{L}_\sigma = \mathrm{diag}(\alpha(\mathcal{L}\otimes I_s), \beta(\mathcal{L}\otimes I_1))$, $\vartheta = \mathrm{col}(x, \bar{r}_1)$, $\Xi = \mathrm{col}(\Upsilon, \Psi)$, $H^1(\vartheta) = h^1(x, \bar{r}_1)$ and $\nabla_\vartheta H^1(\vartheta) = \mathrm{col}(\nabla_x h^1(x, \bar{r}_1), \nabla_{\bar{r}_1} h^1(x, \bar{r}_1))$. Additionally, since $H^1(\vartheta)$ is convex, and $0 < \alpha < \frac{1}{\lambda_{\max}(\mathcal{L})}$ and $0 < \beta < \frac{1}{\lambda_{\max}(\mathcal{L})}$, it results in the positive-definite function V_2.

Based on the strategy (25), since the proximal operator $prox_{h^2}(\cdot)$ has no effect on the variable $\bar{r}_1$, we get

$$\begin{aligned}
&\dot{x} + x = prox_{h^2}[x - \ell - \alpha(\mathcal{L}\otimes I_s)(x - d)],\\
&x^* = prox_{h^2}[x^* - \ell^* - \alpha(\mathcal{L}\otimes I_s)(x^* - d)],\\
&\dot{\bar{r}}_1 + \bar{r}_1 = prox_{h^2}[\bar{r}_1 - \iota - \beta(\mathcal{L}\otimes I_1)\bar{r}_1],\\
&\bar{r}_1^* = prox_{h^2}[\bar{r}_1^* - \iota^* - \beta(\mathcal{L}\otimes I_1)\bar{r}_1^*],
\end{aligned} \tag{28}$$

where $\iota = \nabla_{\bar{r}_1} h^1(x, \bar{r}_1) + \beta(\mathcal{L}\otimes I_1)\Psi$. Furthermore, $h^2(\cdot)$ is convex and its subgradient $\partial h^2(\cdot)$ is monotone. And it follows from (28) that

$$\varkappa^{\mathrm{T}}(\vartheta - \vartheta^* + \dot{\vartheta}) \geqslant 0, \tag{29}$$

where $\varkappa = \nabla_\vartheta H^1(\vartheta^*) - \nabla_\vartheta H^1(\vartheta) - \mathcal{L}_\sigma(\Xi - \Xi^*) - \mathcal{L}_\sigma(\vartheta - \vartheta^*) - \dot{\vartheta}$. With (29), the derivative of V_2 along the strategy (25) satisfies

$$\begin{aligned}
\dot{V}_2 &= (\vartheta - \vartheta^*)\dot{\vartheta} + (\Xi - \Xi^*)\dot{\Xi} + (\nabla_\vartheta H^1(\vartheta) - \nabla_\vartheta H^1(\vartheta^*) + \vartheta^{\mathrm{T}}\mathcal{L}_\sigma)\dot{\vartheta} + \dot{\vartheta}^{\mathrm{T}}\mathcal{L}_\sigma(\Xi - \Xi^*) + \vartheta^{\mathrm{T}}\mathcal{L}_\sigma\dot{\Xi}\\
&\leqslant -\|\dot{\vartheta}\|^2 - \vartheta^{\mathrm{T}}\bar{\mathcal{L}}_\sigma\vartheta - (\nabla_\vartheta H^1(\vartheta) - \nabla_\vartheta H^1(\vartheta^*))^{\mathrm{T}}(\vartheta - \vartheta^*) \leqslant 0,
\end{aligned} \tag{30}$$

where $\bar{\mathcal{L}}_\sigma = \mathcal{L}_\sigma^{\mathrm{T}}(I_{(s+1)m} - \mathcal{L}_\sigma)$.

Since $0 < \alpha < \frac{1}{\lambda_{\max}(\mathcal{L})}$ and $0 < \beta < \frac{1}{\lambda_{\max}(\mathcal{L})}$, it notes that $\lambda_i(\bar{\mathcal{L}}_\sigma) \geqslant 0$, $\forall i \in [(s+1)m]$. Hence,

$$\dot{V}_2 \leqslant -\|\dot{\vartheta}\|^2 - (\nabla_\vartheta H^1(\vartheta) - \nabla_\vartheta H^1(\vartheta^*))^{\mathrm{T}}(\vartheta - \vartheta^*) \leqslant 0. \tag{31}$$

Therefore, the equilibrium point $(x^*, \bar{r}_1^*, \Upsilon^*, \Psi^*)$ is Lyapunov stable and the boundedness of $(x(t), \bar{r}_1(t), \Upsilon(t), \Psi(t))$ is ensured for all $t \in \mathbb{R}^+$.

Define a set $\Theta = \{(x, \bar{r}_1, \Upsilon, \Psi) : \dot{V}_2 = 0\}$. Let $\hat{\Theta}$ be the largest invariant set of Θ. In light of the invariance principle, it holds $\lim_{t\to\infty}(x(t), \bar{r}_1(t), \Upsilon(t), \Psi(t)) \in \hat{\Theta}$. Assume $(\hat{x}(t), \hat{\bar{r}}_1(t), \hat{\Upsilon}(t), \hat{\Psi}(t))$ is a trajectory associated with the strategy (25) such that $(\hat{x}(0), \hat{\bar{r}}_1(0), \hat{\Upsilon}(0), \hat{\Psi}(0)) \in \hat{\Theta}$. Then, $(\hat{x}(t), \hat{\bar{r}}_1(t), \hat{\Upsilon}(t), \hat{\Psi}(t)) \in \hat{\Theta}$ for all $t \geqslant 0$. Therefore, $\dot{\hat{x}}(t) = \mathbf{0}_{sm}$, $\dot{\hat{\bar{r}}}_1(t) = \mathbf{0}_m$, $\dot{\hat{\Upsilon}}(t) = \alpha(\mathcal{L}\otimes I_s)(\hat{x} - d) = C_1$, and $\dot{\hat{\Psi}}(t) = \beta(\mathcal{L}\otimes I_1)\hat{\bar{r}}_1 = C_2$. If $C_1 \neq 0$ and $C_2 \neq 0$, $\hat{\Upsilon}(t)$ and $\hat{\Psi}(t)$ will become infinite, which violates the boundedness of $(\hat{x}(t), \hat{\bar{r}}_1(t), \hat{\Upsilon}(t), \hat{\Psi}(t)) \in \hat{\Theta}$. Hence, $\hat{\Theta} \subseteq \{(x, \bar{r}, \Upsilon, \Psi) : \dot{x} = \mathbf{0}_{sm}, \dot{\bar{r}} = \mathbf{0}_m, \dot{\Upsilon} = \mathbf{0}_{sm}, \dot{\Psi} = \mathbf{0}_m\}$. Because any point in the set $\hat{\Theta}$ is Lyapunov stable, the trajectory $(x(t), \bar{r}(t), \Upsilon(t), \Psi(t))$ converges to an equilibrium point of (25) [27]. According to Lemma 4, $(x(t), \bar{r}(t))$ converges to the optimal solution of the optimization problem (22).

An RNE searching algorithm is presented in Algorithm 1. The algorithm has two steps. In step 1, based on the distributed continuous-time NE seeking strategy (6), the states x_i, $\forall i \in [m]$, are able to search for an NE point. We select a maximal time T_1, such that $\|x_i(T_1) - x_i(T_1 - 1)\| \leqslant o$, $\forall i \in [m]$, with a small enough tolerance error o. Next, an extra process is employed to assess whether the common state constraint is loose enough. Actually, when the common state constraint is loose enough, the optimal formation configuration searched by the strategy (6) is the predefined one for the multi-agent system, such that $x_i - d_i - x_k + d_k = 0$, $\forall i, k \in [m]$. It results in the cost function $J_i = 0$, $\forall i \in [m]$. Thus, the following two representations are equivalent. (1) The common state constraint is loose enough. (2) The optimal formation configuration searched by strategy (6) holds $\sum_{i=1}^m J_i = 0$. Thus, a reasonable way to judge whether the common state constraint is loose enough is to assess whether $\sum_{i=1}^m J_i = 0$. If $\|\frac{\sum_{i=1}^m J_i(x_i(T_1), e_1\chi_i(T_1), e_2\chi_i(T_1))}{m}\| > o_1$ with a small enough tolerance error o_1, we believe that the state constraint is tight, and output the uniqueness of the NE point, $x_i(T_1)$, as the RNE point. However, since the global cost function is unavailable for each agent in a distributed communication topology, an observer similar to (6) for each agent is designed as

$$\begin{aligned}
&\dot{\xi}_i = -\xi_i + \sum_{j=1}^m a_{ij}(\xi_i - \xi_j) + \sum_{j=1}^m a_{ij}(\kappa_i - \kappa_j) + J_i(T_1),\\
&\dot{\kappa}_i = \xi_i,\ \forall i \in [m],
\end{aligned} \tag{32}$$

where $J_i(T_1)$ is the abbreviation of $J_i(x_i(T_1), e_1\chi_i(T_1), e_2\chi_i(T_1))$. When the agents access the common state constraint is loose enough, the strategy (25) is proposed to iterate the states x_i in step 2. Similarly, we select a maximal time T_2 such that $\|x_i(T_2) - x_i(T_2 - 1)\| \leqslant o$ and output $x_i(T_2)$ as the RNE.

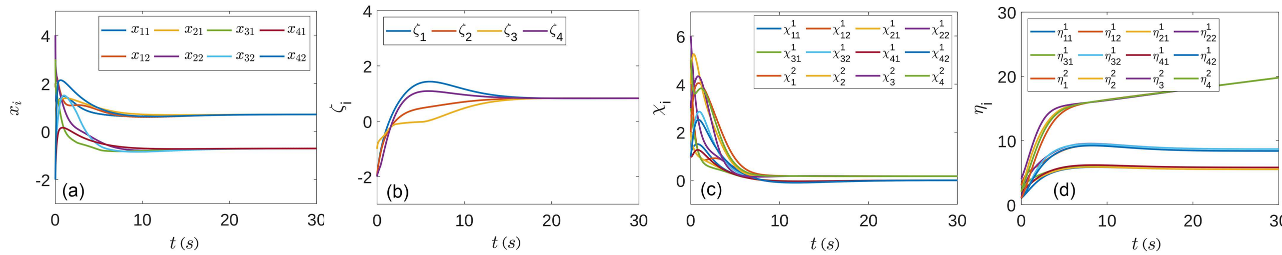

Figure 1 (Color online) Evolutions of the variables about NE point searching with a tight state constraint. (a) x_i; (b) ζ_i; (c) χ_i; (d) η_i.

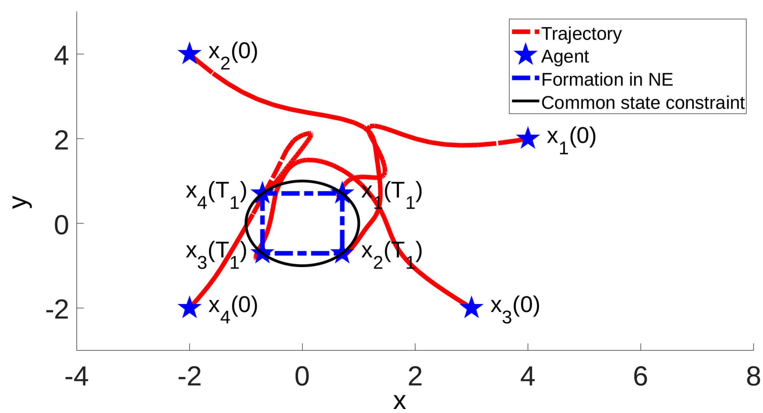

Figure 2 (Color online) The trajectory to an NE point with a tight state constraint.

Algorithm 1 RNE searching algorithm with a general constraint.

Step 1 NE point searching:
Give the desired formation configuration d_i, and the common constraint Ω;
Initialize the variables $x_i(0)$, $\chi_i(0)$, $\eta_i(0)$ and $\zeta_i(0)$ and iterate the strategy (6);
Output the NE point $x_i(T_1)$ as the RNE point if the common state constraint is not loose; otherwise, go to step 2;
Step 2 RNE point searching:
Initialize the variables $r_{1i}(0)$, $\upsilon_i(0)$, $\psi_i(0)$, and $\tau(0)$ and iterate the strategy (25) with $x_i(0) = x_i(T_1)$;
Output $x_i(T_2)$ as the RNE point.

Remark 9. Compared with the algorithms in [12,14,15] which only focus on NE searching, the proposed algorithm in this paper analyzes the uniqueness of the NE point further, meanwhile, searches for the RNE point, which has the maximal robust ability.

5 Simulations

In this section, two simulation examples are provided to validate our proposed algorithms with a quadratic constraint set and a general constraint set, respectively. In these two examples, a multi-agent system consists of 4 agents under a distributed communication topology, whose Laplacian matrix satisfies

$$\mathcal{L} = \begin{bmatrix} 2 & -1 & 0 & -1 \\ -1 & 2 & -1 & 0 \\ 0 & -1 & 2 & -1 \\ -1 & 0 & -1 & 2 \end{bmatrix}. \tag{33}$$

The predefined formation is designed as $d = [1,1,-1,-1,1,-1,-1,1]^{\mathrm{T}}$ and initial states of agents as $x(0) = [4,-2,3,-2,2,4,-2,-2]^{\mathrm{T}}$.

Example 1. First, we consider a tight state constraint $\Omega_{tight} = \{x_f | (x_f - \bar{x}_{tight})^{\mathrm{T}}(x_f - \bar{x}_{tight}) - r_{tight}^2 \leqslant 0\}$ with $\bar{x}_{tight} = [0;0]$ and $r_{tight} = 1$. Based on the strategy (6), the evolutions of variables x_i, ζ_i, χ_i and η_i are shown in Figures 1(a)–(d), respectively. It is worth noting that the variable ζ_i converges to a positive constant in Figure 1(b), which represents the influence of the active constraint on each agent, and the variables χ_i and η_i are related to the estimator of the aggregate item, shown in Figures 1(c) and (d). Figure 2 illustrates the

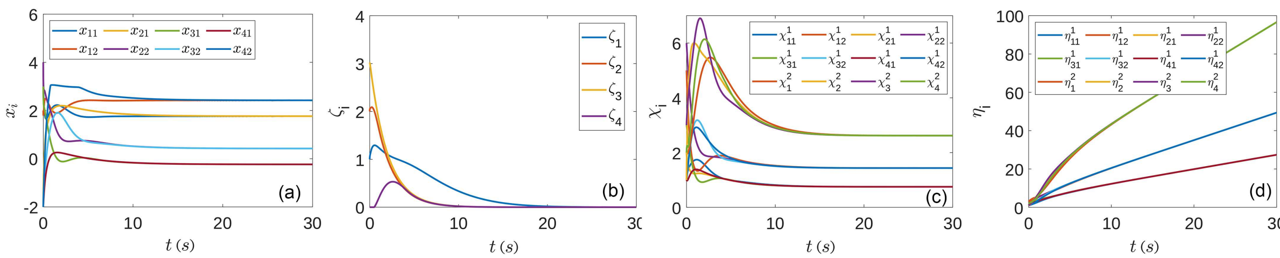

Figure 3 (Color online) Evolutions of the variables about NE point searching with a loose state constraint. (a) x_i; (b) ζ_i; (c) χ_i; (d) η_i.

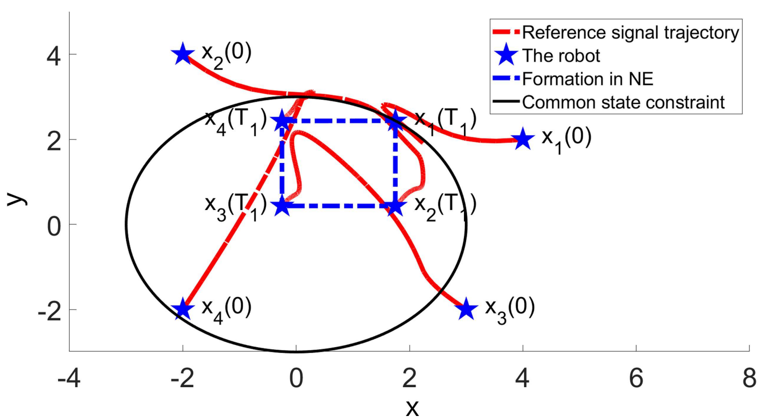

Figure 4 (Color online) The trajectory to an NE point with a loose state constraint.

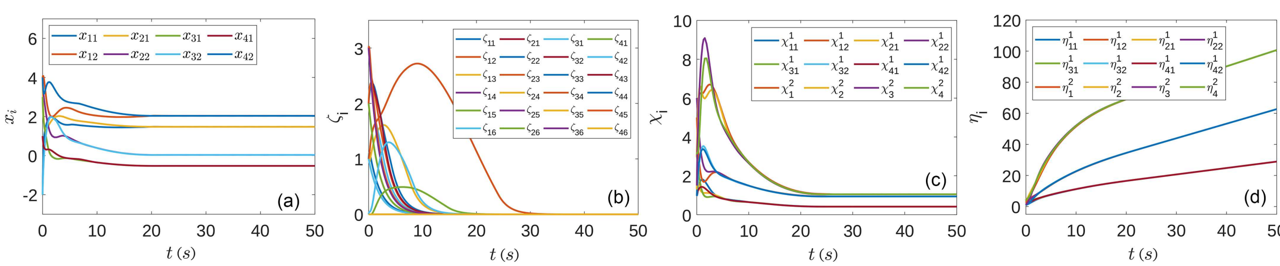

Figure 5 (Color online) Evolutions of the variables about NE point searching with a general constraint. (a) x_i; (b) ζ_i; (c) χ_i; (d) η_i.

agents' trajectories. Obviously, to accommodate within the tight constraint Ω_{tight}, the multi-agent system changes its formation configuration adaptively with the minimal formation change. Furthermore, when we choose a loose enough state constraint $\Omega_{loose} = \{x_f | (x_f - \bar{x}_{loose})^{\mathrm{T}}(x_f - \bar{x}_{loose}) - r_{loose}^2 \leqslant 0\}$ with $\bar{x}_{loose} = [0; 0]$ and $r_{loose} = 3$, based on the strategy (6), the evolutions of the variables x_i, ζ_i, χ_i and η_i are illustrated in Figure 3. Specially, in Figure 3(b), the variable ζ_i converges to zero, because the state constraint is loose enough to be inactive and does not impose any force on the agent. Furthermore, the agents' trajectories to search for an NE point are shown in Figure 4. Obviously, the multi-agent system in the NE point forms the predefined formation configuration. As previously analyzed, the NE point is near to the boundary of the state constraint.

Example 2. A general convex set is defined as $\Omega_{general} = \{\mathbf{x} | A\mathbf{x} + B \leqslant 0\}$, where $A = \begin{bmatrix} -1.5 & 0.5 & 2 & 1.5 & -0.5 & -2 \\ 1 & 1 & 1 & -1 & -1 & -1 \end{bmatrix}^{\mathrm{T}}$ and $B = [-3\ -3\ -6\ -4.5\ -2.5\ -4]^{\mathrm{T}}$. Based on step 1 in Algorithm 1, the evolutions of the variables x_i, ζ_i, χ_i and η_i of the strategy (6) are shown in Figure 5. The trajectories of agents converging to an NE point are presented in Figure 6. It is worth noting that all agents enter into the general convex set $\Omega_{general}$ and maintain the pre-described formation configuration finally, because the general state constraint is loose enough. According to step 2 of Algorithm 1 with $\tau = 50$ and $\alpha = \beta = 0.22$, the simulation results about the variables x_i, r_{1i}, υ_i and ψ_i are shown in Figures 7(a)–(d), respectively. The trajectories of agents starting from the NE point are illustrated in Figure 8(a). The multi-agent system converges to an RNE point finally, which is located on the core of the common state constraint set $\Omega_{general}$. Furthermore, to verify that the strategy (25) is not affected by different NE points, we choose another NE point as the initial state and search for the RNE based on step 2 of Algorithm 1 with the same parameters. The trajectories of agents are illustrated in Figure 8(b). It is obvious that starting from different NEs,

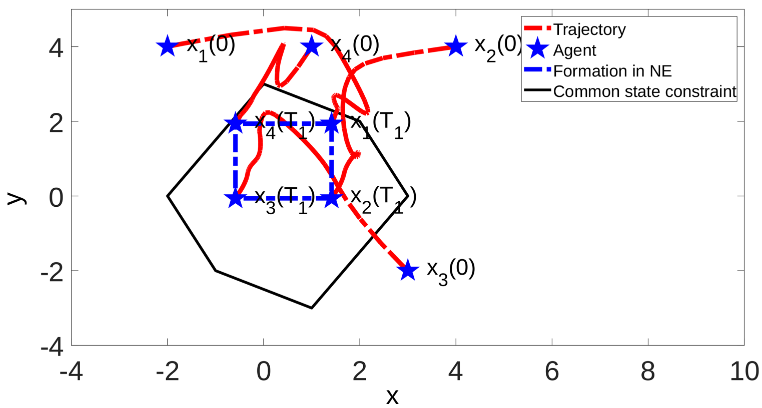

Figure 6 (Color online) The trajectory to an NE point with a general constraint.

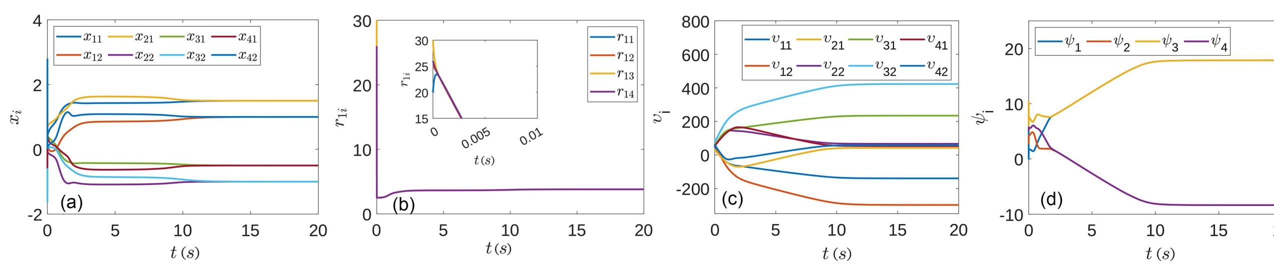

Figure 7 (Color online) Evolutions of the variables about RNE searching with a general constraint. (a) x_i; (b) r_{1i}; (c) v_i; (d) ψ_i.

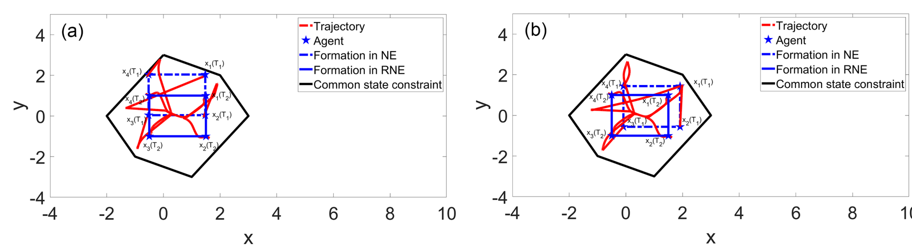

Figure 8 (Color online) The simulation results of RNE searching. (a) Case 1; (b) case 2.

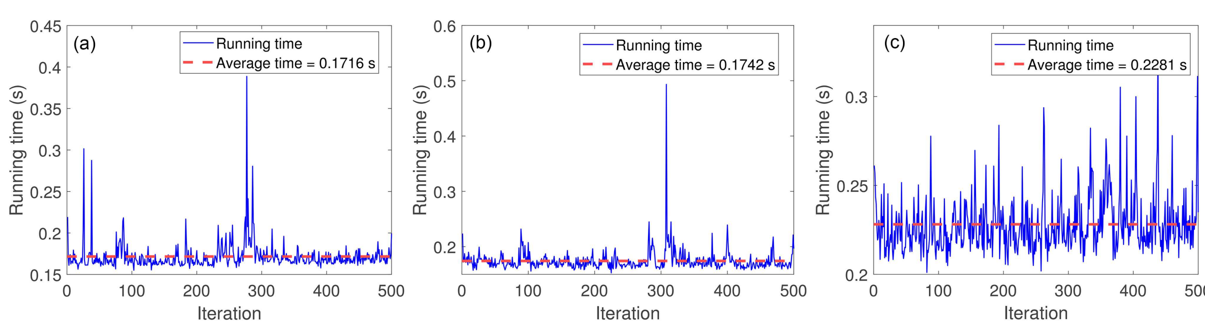

Figure 9 (Color online) The iteration time for the distributed continuous-time NE seeking strategy (6) under different common state constraints. (a) 3 inequality constraints; (b) 6 inequality constraints; (c) 9 inequality constraints.

the states of the multi-agent system both converge to RNE finally. It implies that the convergence of the strategy (25) is not affected by different NE points.

Additionally, to analyze the impact of high-dimensional variables in the distributed continuous-time NE seeking strategy (6), we select 3 sets of different common state constraints, including 3, 6, and 9 inequality constraints, respectively. We test 500 iterations for the strategy (6) under these different common state constraints, using Intel(R) Core(TM) i7-7500U CPU @ 2.70 GHz, and calculate the average time. These simulation results are shown in Figure 9. Obviously, as the number of inequality constraints increases, the dimension of Lagrangian multipliers increases. It results in time complexity and average iteration time increasing. Furthermore, we test the average

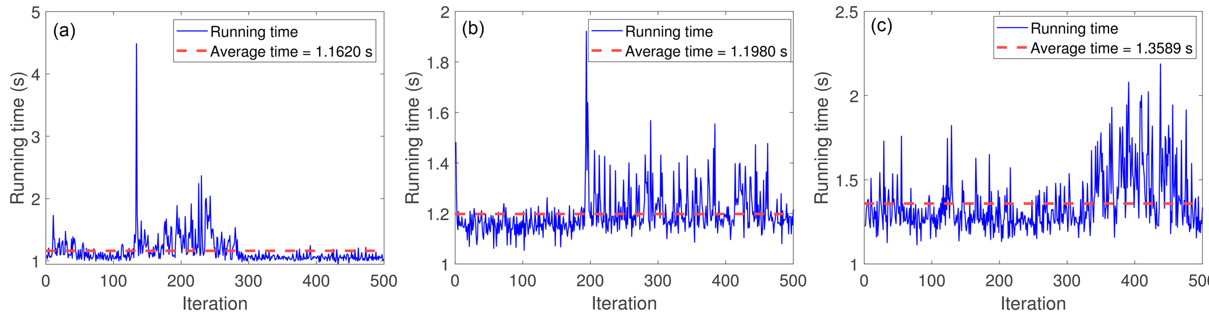

Figure 10 (Color online) The iteration time for the projection method under different common state constraints. (a) 3 inequality constraints; (b) 6 inequality constraints; (c) 9 inequality constraints.

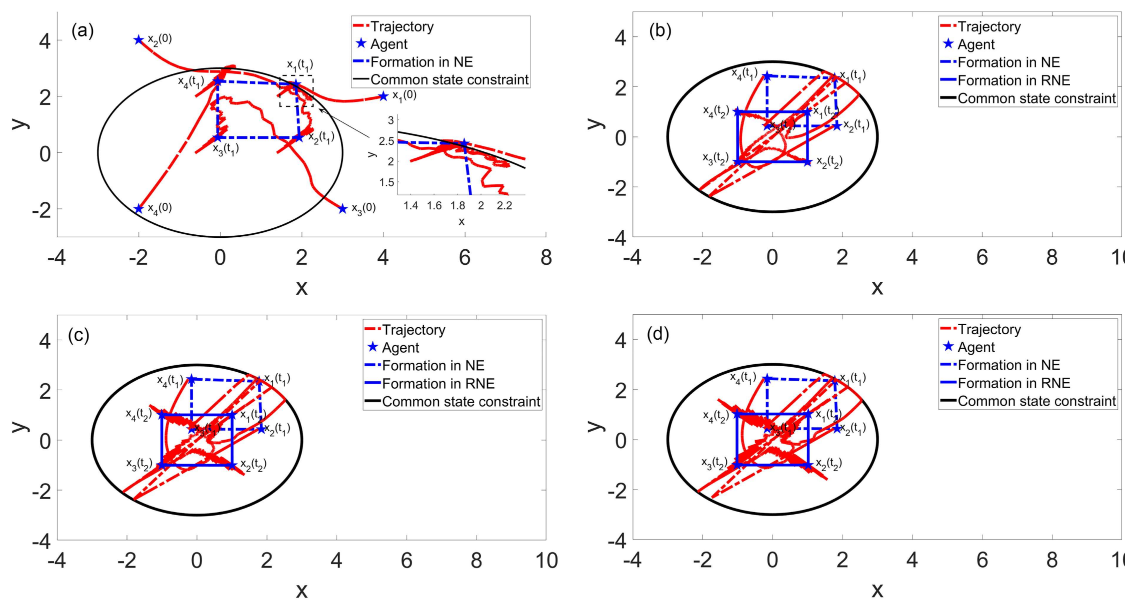

Figure 11 (Color online) The trajectories for the multi-agent system with model uncertainty. (a) NE searching with $\omega_i \sim N(0,1)$; (b) RNE searching with $\omega_i \sim N(0,1)$; (c) RNE searching with $\omega_i \sim N(0,10)$; (d) RNE searching with $\omega_i \sim N(0,20)$.

time for the projection method [13] under these 3 sets of different common state constraints. The simulation results are described in Figure 10. It is worth noting that time complexity and average iteration time also increase with the increasing number of inequality constraints. Furthermore, the average iteration time of the projection method is longer than that of the Lagrangian method, because the projection method requires an additional quadratic optimization problem to find suitable projection points, but the convergence rate of the projection method is faster than that of the Lagrange method, because it can quickly project the state of the agent inside the common constraints.

Furthermore, to display the robust performance of the RNE, we add an uncertainty to the model, such that $\dot{x}_i = u_i + \omega_i,\ i \in [4]$, where ω_i is normally distributed. In Figure 11(a), it displays the trajectory for the multi-agent system based on the distributed continuous-time NE seeking strategy (6) in the loose enough state constraint case described in Example 1, where the uncertainty $\omega_i \sim N(0,1),\ i \in [4]$. It is seen that the trajectory of the multi-agent system fluctuates because of the uncertainty of the model. Since the NE point searched by the strategy (6) is close to the boundary of the common state constraint, the final formation configuration for the multi-agent system is affected by disturbances and deviates from the common state constraint, as shown in the enlarged view in Figure 11(a). Furthermore, Figure 11(b) shows the trajectory for the multi-agent system based on the strategy (25). Because RNE is far away from the boundary of the common state constraint, the multi-agent system can be maintained within the common state constraint in the presence of uncertainty in the model, ensuring the security of the system. Additionally, in the process of searching for RNE, we choose two sets of larger uncertainties imposed on the model, and the trajectories for the multi-agent system are shown in Figures 11(c) and (d), where $\omega_i \sim N(0,10)$ and $\omega_i \sim N(0,20),\ i \in [4]$, respectively. Obviously, with the increase of model uncertainty, there is a significant increase in trajectory jitter, but the state of the multi-agent system still remains within the common state constraint, because of a large distance from the boundary for the RNE.

6 Conclusion

In this article, an adaptive constrained formation problem has been regarded as an aggregative game to optimize the formation configuration change further. Then, a distributed continuous-time NE seeking strategy has been proposed to search for an NE point of the aggregative game. Interestingly, the number of the NE points depends on the size of the security region established by the common state constraint set. Furthermore, we have considered an extra property of NE points and first introduced the concept of RNE. An RNE searching algorithm has been provided for the RNE point in a general but convex constraint. In the future, we will further analyze more properties of NE points and design the RNE search algorithm under the full distributed structure.

Acknowledgements This work was supported by Fundamental Research Funds for the Central Universities (Grant No. YWF-22-L-631) and National Natural Science Foundation of China (Grant No. 62576223).

References

1 Yan T, Xu Z, Yang S X, et al. Formation control of multiple autonomous underwater vehicles: a review. Intell Robot, 2023, 3: 1–22
2 Wu B, Peng Z, Wen G, et al. Distributed constrained optimal formation matching for large-scale systems. IEEE Trans Automat Contr, 2024, 69: 3457–3464
3 Jia R R, Zong X F, Wang Q. Time-varying formation tracking control of high-order multi-agent systems with multiple leaders and multiplicative noise. Sci China Inf Sci, 2024, 67: 222203
4 Liu Y, Huang P, Zhang F, et al. Distributed formation control using artificial potentials and neural network for constrained multiagent systems. IEEE Trans Contr Syst Technol, 2020, 28: 697–704
5 Lashkari N, Biglarbegian M, Yang S X. Development of a novel robust control method for formation of heterogeneous multiple mobile robots with autonomous docking capability. IEEE Trans Automat Sci Eng, 2020, 17: 1759–1776
6 Tsang K F E, Huang M, Shi L, et al. Stochastic event-triggered algorithm for distributed convex optimization. IEEE Trans Control Netw Syst, 2023, 10: 1374–1386
7 Yang S F, Xu W Y, He W L, et al. Distributed generalized Nash equilibrium seeking: event-triggered coding-decoding-based secure communication. Sci China Inf Sci, 2024, 67: 172205
8 Tian F, Yu W, Fu J, et al. Distributed optimization of multiagent systems subject to inequality constraints. IEEE Trans Cybern, 2021, 51: 2232–2241
9 Zhang D, Wang Y, Meng L, et al. Adaptive critic design for safety-optimal FTC of unknown nonlinear systems with asymmetric constrained-input. ISA Trans, 2024, 155: 309–318
10 Qin C, Qiao X, Wang J, et al. Barrier-critic adaptive robust control of nonzero-sum differential games for uncertain nonlinear systems with state constraints. IEEE Trans Syst Man Cyber Syst, 2024, 54: 50–63
11 Barrera J, Garcia A. Dynamic incentives for congestion control. IEEE Trans Automat Contr, 2015, 60: 299–310
12 Salehisadaghiani F, Pavel L. Distributed Nash equilibrium seeking: a gossip-based algorithm. Automatica, 2016, 72: 209–216
13 Liang S, Yi P, Hong Y. Distributed Nash equilibrium seeking for aggregative games with coupled constraints. Automatica, 2017, 85: 179–185
14 Bakhshayesh B G, Kebriaei H. Decentralized equilibrium seeking of joint routing and destination planning of electric vehicles: a constrained aggregative game approach. IEEE Trans Intell Transp Syst, 2022, 23: 13265–13274
15 Zhu Y, Yu W, Wen G, et al. Distributed Nash equilibrium seeking in an aggregative game on a directed graph. IEEE Trans Automat Contr, 2021, 66: 2746–2753
16 Léchappé V, Moulay E, Plestan F, et al. New predictive scheme for the control of LTI systems with input delay and unknown disturbances. Automatica, 2015, 52: 179–184
17 Miranda-Villatoro F A, Castanos F. Robust output regulation of strongly passive linear systems with multivalued maximally monotone controls. IEEE Trans Automat Contr, 2017, 62: 238–249
18 Kolarijani A S, Bregman S C, Esfahani P M, et al. A decentralized event-based approach for robust model predictive control. IEEE Trans Automat Contr, 2020, 65: 3517–3529
19 Bertsimas D, Sim M. The price of robustness. Operations Res, 2004, 52: 35–53
20 Ben-Tal A, Nemirovski A. Robust solutions of uncertain linear programs. Operations Res Lett, 1999, 25: 1–13
21 Wu S, Ren X, Hong Y, et al. Max-min fair sensor scheduling: game-theoretic perspective and algorithmic solution. IEEE Trans Automat Contr, 2021, 66: 2379–2385
22 Peng Z N, Hu J P, Ghosh B K. Data-driven containment control of discrete-time multi-agent systems via value iteration. Sci China Inf Sci, 2020, 63: 189205
23 Zhang H, Yue D, Dou C, et al. Two-layered hierarchical optimization strategy with distributed potential game for interconnected hybrid energy systems. IEEE Trans Cybern, 2023, 53: 5436–5447
24 Boyd S, Vandenberghe L. Convex Optimization. Cambridge: Cambridge University Press, 2004
25 Cheng D, Wang J, Hu X. An extension of LaSalle's invariance principle and its application to multi-agent consensus. IEEE Trans Automat Contr, 2008, 53: 1765–1770
26 Derenick J C, Spletzer J R. Convex optimization strategies for coordinating large-scale robot formations. IEEE Trans Robot, 2007, 23: 1252–1259
27 Wei Y, Fang H, Zeng X, et al. A smooth double proximal primal-dual algorithm for a class of distributed nonsmooth optimization problems. IEEE Trans Automat Contr, 2020, 65: 1800–1806